



Research paper

Structural diversity in cobalt camphorate coordination polymers with flexible dipyridylamide ligands including looped layers and self-penetrated topologies

Jack J. Przybyła, Frederick C. Ezenyilimba, Robert L. LaDuca*

Lyman Briggs College and Department of Chemistry, Michigan State University, East Lansing, MI 48825, USA

ARTICLE INFO

Keywords:

Crystal structure
Coordination polymer
Cobalt
Self-penetration
Interpenetration

ABSTRACT

Hydrothermal reaction of cobalt nitrate, *D*-camphoric acid, and flexible dipyridylamide ligands afforded a series of coordination polymers with diverse structural topologies, as characterized by single crystal X-ray diffraction. $\{[\text{Co}_2(\text{DL-cam})_2(\text{edn})]\cdot 2\text{H}_2\text{O}\}_n$ (1, edn = *N,N'*-(ethane-1,2-diyl)dinicotinamide) shows a 3D $4^{12}6^3$ **pcu** net built from straight-pillaring of $\{\text{Co}_2(\text{OCO})_4\}$ paddlewheel dimer-based $[\text{Co}_2(\text{DL-cam})_2]_n$ layer motifs. In contrast, $[\text{Co}(\text{D-cam})(\text{edin})]_n$ (2, edin = *N,N'*-(ethane-1,2-diyl)diisonicotinamide) manifests a two-fold parallel interpenetrated looped layer topology. $\{[\text{Co}_2(\text{DL-cam})_2(\text{bdin})]\cdot 2\text{H}_2\text{O}\}_n$ (3, bdin = *N,N'*-(butane-1,4-diyl)diisonicotinamide) displays a very rare 3D $4^46^{10}8$ **roa** self-penetrated net built from cross-pillaring of $\{\text{Co}_2(\text{OCO})_4\}$ paddlewheel dimer-based $[\text{Co}_2(\text{DL-cam})_2]_n$ layer motifs, as does $\{[\text{Co}_2(\text{DL-cam})_2(\text{pedin})]\cdot 2\text{H}_2\text{O}\}_n$ (4, pedin = *N,N'*-(pentane-1,5-diyl)diisonicotinamide). $[\text{Co}(\text{D-cam})(\text{hdin})]_n$ (5, hdin = *N,N'*-(hexane-1,6-diyl)diisonicotinamide) shows a simple stacked system of sawtooth (4,4) grid motifs. Thermal properties are discussed herein.

1. Introduction

Investigations towards the preparation, structural characterization, and property measurements of crystalline divalent metal coordination polymer networks remain intense in many research groups around the world. This intriguing class of materials possesses exciting applications in hydrogen storage [1], molecular absorption [2], ion exchange [3], heterogeneous catalysis for organic transformations [4], second harmonic generation [5], explosives trace detection [6], and even delivery of active pharmaceuticals [7]. Chiral coordination polymers can be employed in enantioselective separations or stereospecific organic transformations [8]. Lin's group reported using a chiral dipyridyl linking ligand to prepare a two-fold interpenetrated cadmium coordination polymer that can catalyze the stereospecific formation of chiral secondary alcohols from aromatic aldehydes in the presence of diethyl zinc, after post-synthetic reaction with titanium isopropoxide [8a]. Rosseinsky's group employed the conjugate base of the amino acid *L*-aspartic acid (*L*-aspH) as the carboxylate ligand to form the 3D chiral phase $[\text{Ni}_2(\text{L-asp})_2(\text{bpy})]_n$ (bpy = 4,4'-bipyridine), which can perform gas phase enantiospecific separation of aliphatic diols [8b].

The *D*-camphorate ligand (*D*-cam, Scheme 1) has shown to be an excellent ligand for promoting the formation of chiral divalent metal coordination networks, either in the presence [9] or the absence [10] of

a neutral dipyridyl coligand. Bu's group reported the synthesis and characterization of three distinct 3-D cadmium *D*-camphorate phases by varying temperature conditions [10]. Control of dimensionality can be achieved by varying the divalent metal ion with the more conformationally flexible coligand 1,3-di-4-pyridylpropane (dpp). $[\text{Ni}(\text{D-cam})(\text{dpp})]_n$ showed an unusual chiral bilayer structure with 4^26^38 topology, while its cobalt congener $\{[\text{Co}(\text{D-cam})(\text{dpp})]\cdot \text{H}_2\text{O}\}_n$ manifests a chiral three-fold interpenetrated diamondoid net [9a]. $\{[\text{Cd}(\text{D-cam})(\text{dpp})]\cdot 2\text{H}_2\text{O}\}_n$ has a similar diamondoid topology to $\{[\text{Co}(\text{D-cam})(\text{dpp})]\cdot \text{H}_2\text{O}\}_n$, and also undergoes a thermally induced single crystal-to-single crystal structural reorganization [9b].

Employing the "V-shaped" and hydrogen-bonding capable coligand 4,4'-dipyridylamine (dpa), our group prepared a series of chiral *D*-camphorate coordination polymers with structural topologies dependent on the nature of the divalent metal ion [11]. $\{[\text{Cd}(\text{dpa})(\text{D-cmphH})_2(\text{H}_2\text{O})]\cdot 0.875\text{H}_2\text{O}\}_n$ possessed 1D helical chains with a very long pitch of over 67 Å. $[\text{Zn}_2(\text{D-cmph})_2(\text{dpa})(\text{H}_2\text{O})]_n$ showed a 2D 3,4-connected binodal net with a rare $(5^3)_2(5^48^2)$ topology. $\{[\text{Ni}(\text{D-cmph})(\text{dpa})]\cdot 3\text{H}_2\text{O}\}_n$ showed an uncommon 2-fold interpenetrated 4-connected 3D 4^28^4 **lvt** topology, while its cobalt analog $[\text{Co}_2(\text{D-cmph})_2(\text{dpa})]\cdot \text{H}_2\text{O}\}_n$ possessed a $4^{12}6^3$ **pcu** topology based on 6-connected $\{\text{Co}_2(\text{OCO})_4\}$ paddlewheel dimers. Other hydrogen-bonding capable and conformationally flexible dipyridyl ligands allowed access

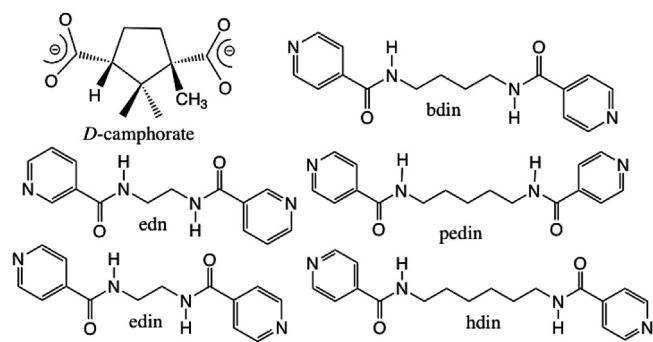
* Corresponding author.

E-mail address: laduca@msu.edu (R.L. LaDuca).<https://doi.org/10.1016/j.ica.2019.119087>

Received 5 August 2019; Received in revised form 20 August 2019; Accepted 21 August 2019

Available online 29 August 2019

0020-1693/© 2019 Elsevier B.V. All rights reserved.



Scheme 1.

to a diverse of structural topologies in cobalt camphorate coordination polymers, sometimes with scrambling of the original *D*-camphorate chirality [12]. $\{[\text{Co}_2(\text{DL-cam})_2(\text{bdn})]\cdot 2\text{H}_2\text{O}\}_n$ (**1**, bdn = *N,N'*-(butane-1,4-diyl)dinicotinamide) possesses $\{\text{Co}_2(\text{OCO})_4\}$ paddlewheel dimer-based chirality-scrambled $[\text{Co}_2(\text{DL-cam})_2]$ grid layers pillared by bdn ligands into a 6-connected $4^{12}6^3$ **pcu** network, similar in topology to the dpa derivative $[\text{Co}_2(\text{D-cmph})_2(\text{dpa})]\cdot \text{H}_2\text{O}\}_n$. The shorter dipyriddyamide *N,N'*-(propane-1,3-diyl)dinicotinamide (pdn) afforded $\{[\text{Co}_2(\text{D-cam})_2(\text{pdn})]\cdot 2\text{H}_2\text{O}\}_n$. In contrast to the **pcu** straight-pillared topology of the bdn-containing analog, this pdn-containing phase manifests a cross-pillared self-penetrated 4^46^810 **mab** network along with retention of chirality. $\{[\text{Co}_2(\text{DL-cam})_2(\text{pedn})]\cdot 2\text{H}_2\text{O}\}_n$ (pedn = *N,N'*-(pentane-1,5-diyl)dinicotinamide) shows a highly crystallographically disordered hybrid structure of discrete slabs of 3D **pcu** network with interleaved 2D **hxl** (3,6) layers at random intervals, instead of the self-penetrated **mab** network seen in the pdn-containing derivative. Thus the length of the dipyriddyamide aliphatic unit can play an extremely significant role in structure direction among cobalt camphorate coordination polymers.

We have intended in this study to expand the scope of our previous work and prepare additional chiral cobalt *D*-camphorate coordination networks with hydrogen-bonding capable and conformationally flexible dipyriddydicotinamide and dipyriddyisonicotinamide ligands. In this contribution we present the synthesis, single-crystal structures, topological analysis, and thermal properties of $\{[\text{Co}_2(\text{DL-cam})_2(\text{edn})]\cdot 2\text{H}_2\text{O}\}_n$ (**1**, edn = *N,N'*-(ethane-1,2-diyl)dinicotinamide, Scheme 1), $[\text{Co}(\text{D-cam})(\text{edin})]_n$ (**2**, edin = *N,N'*-(ethane-1,2-diyl)diisonicotinamide, Scheme 1), $\{[\text{Co}_2(\text{DL-cam})_2(\text{bdn})]\cdot 2\text{H}_2\text{O}\}_n$ (**3**, bdn = *N,N'*-(butane-1,4-diyl)diisonicotinamide, Scheme 1), $\{[\text{Co}_2(\text{DL-cam})_2(\text{pedin})]\cdot 2\text{H}_2\text{O}\}_n$ (**4**, pedin = *N,N'*-(pentane-1,5-diyl)diisonicotinamide, Scheme 1), and $[\text{Co}(\text{D-cam})(\text{hdin})]_n$ (**5**, hdin = *N,N'*-(hexane-1,6-diyl)diisonicotinamide, Scheme 1).

2. Experimental section

2.1. General considerations

Cobalt nitrate and *D*-camphoric acid were commercially obtained from Sigma Aldrich. *N,N'*-(ethane-1,2-diyl)dinicotinamide (edn) was prepared by condensation of 1,2-ethanediamine and two molar equivalents of nicotinoyl chloride hydrochloride in dry pyridine. The reaction mixture was quenched with water, and then the product was isolated via CH_2Cl_2 extraction and removal of solvent *in vacuo* [13]. Other dipyriddyamides were prepared similarly by using the requisite diamines and isonicotinoyl chloride hydrochloride in dry pyridine. Water was deionized above $3\text{M}\Omega\text{-cm}$ in-house. IR spectra were recorded on powdered samples using a Perkin Elmer Spectrum One DRIFT instrument. Thermogravimetric analysis was performed on a TA Instruments Q-50 Thermogravimetric Analyzer with a heating rate of $10^\circ\text{C}/\text{min}$ up to 600°C . Elemental Analysis was carried out using a Perkin Elmer 2400 Series II CHNS/O Analyzer.

Table 1
Crystal and Structure Refinement Data for **1–5**.

Data	1	2
Empirical Formula	$\text{C}_{34}\text{H}_{46}\text{Co}_2\text{N}_4\text{O}_{12}$	$\text{C}_{24}\text{H}_{28}\text{CoN}_4\text{O}_6$
Formula Weight	820.61	527.43
Crystal system	monoclinic	monoclinic
Space group	$P2_1/c$	$P2_1$
<i>a</i> (Å)	10.1393(17)	10.655(7)
<i>b</i> (Å)	13.651(2)	10.152(7)
<i>c</i> (Å)	13.221(2)	11.788(8)
α (°)	90	90
β (°)	97.637(2)	112.724(10)
γ (°)	90	90
<i>V</i> (Å ³)	1813.7(5)	1176.2(14)
<i>Z</i>	2	2
<i>D</i> (g cm ⁻³)	1.503	1.489
μ (mm ⁻¹)	0.982	0.778
Min./max. transmission	0.9148	0.7279
<i>hkl</i> ranges	$-12 \leq h \leq 12,$ $-16 \leq k \leq 16,$ $-15 \leq l \leq 15$	$-12 \leq h \leq 12,$ $-12 \leq k \leq 12,$ $-14 \leq l \leq 15$
Total reflections	14,046	8762
Unique reflections	3326	4227
<i>R</i> (int)	0.0566	0.2215
Parameters	245	259
<i>R</i> ₁ (all data)	0.0671	0.2480
<i>R</i> ₁ (<i>I</i> > 2σ(<i>I</i>))	0.0607	0.1166
w <i>R</i> ₂ (all data)	0.1633	0.3138
w <i>R</i> ₂ (<i>I</i> > 2σ(<i>I</i>))	0.1597	0.2378
Max/min residual (e ⁻ /Å ³)	1.403/−0.471	1.048/−1.359
G.O.F.	1.104	0.946

Data	3	4	5
Empirical Formula	$\text{C}_{36}\text{H}_{50}\text{Co}_2\text{N}_4\text{O}_{12}$	$\text{C}_{37}\text{H}_{52}\text{Co}_2\text{N}_4\text{O}_{12}$	$\text{C}_{28}\text{H}_{34}\text{CoN}_4\text{O}_6$
Formula Weight	848.66	862.68	581.54
Crystal system	monoclinic	monoclinic	orthorhombic
Space group	$P2_1/c$	$P2_1/c$	$P2_12_12$
<i>a</i> (Å)	22.681(7)	12.5972(10)	20.518(4)
<i>b</i> (Å)	12.340(4)	23.6951(19)	9.241(2)
<i>c</i> (Å)	13.694(4)	13.4045(11)	15.071(3)
α (°)	90	90	90
β (°)	90.146(4)	90.2670(10)	90
γ (°)	90	90	90
<i>V</i> (Å ³)	3833(2)	4001.1(6)	2857.7(11)
<i>Z</i>	4	4	4
<i>D</i> (g cm ⁻³)	1.471	1.432	1.352
μ (mm ⁻¹)	0.932	0.894	0.648
Min./max. transmission	0.9029	0.8696	0.9109
<i>hkl</i> ranges	$-27 \leq h \leq 27,$ $-14 \leq k \leq 14,$ $-16 \leq l \leq 16$	$-15 \leq h \leq 15,$ $-28 \leq k \leq 28,$ $-16 \leq l \leq 16$	$-24 \leq h \leq 24,$ $-11 \leq k \leq 11,$ $-18 \leq l \leq 18$
Total reflections	30,253	32,117	23,350
Unique reflections	7014	7348	5310
<i>R</i> (int)	0.0556	0.0633	0.0724
Parameters	501	462	290
<i>R</i> ₁ (all data)	0.1089	0.1365	0.1380
<i>R</i> ₁ (<i>I</i> > 2σ(<i>I</i>))	0.0812	0.0926	0.1025
w <i>R</i> ₂ (all data)	0.1752	0.2924	0.2800
w <i>R</i> ₂ (<i>I</i> > 2σ(<i>I</i>))	0.1649	0.2587	0.2582
Max/min residual (e ⁻ /Å ³)	0.815/−0.397	1.745/−0.979	0.730/−0.908
G.O.F.	1.199	1.049	1.053

2.2. Preparation of $\{[\text{Co}_2(\text{DL-cam})_2(\text{edn})]\cdot 2\text{H}_2\text{O}\}_n$ (**1**)

$\text{Co}(\text{NO}_3)_2\cdot 6\text{H}_2\text{O}$ (107 mg, 0.37 mmol), *D*-camphoric acid (73 mg, 0.37 mmol), and edn (99 mg, 0.37 mmol), and 0.75 mL of a 1.0 M NaOH solution were mixed with 10 mL of distilled H_2O in a 23 mL Teflon-lined acid digestion bomb. The bomb was sealed and heated in an oven at 120°C for 48 h, and then was cooled slowly to 25°C . Magenta crystals

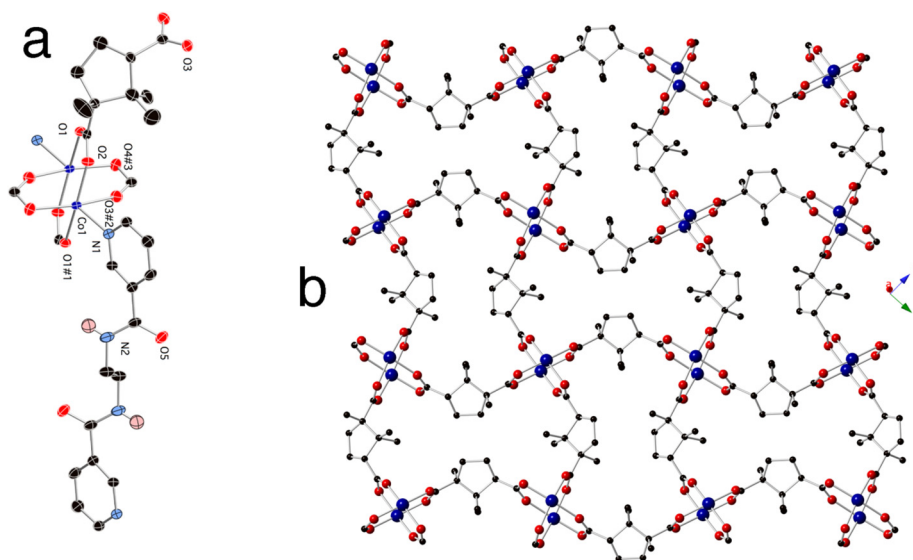


Fig. 1. a) $\{\text{CoNO}_4\}$ square pyramidal coordination environment, $\{\text{Co}_2(\text{CO}_2)_4\}$ paddlewheel dimeric unit and complete ligand set in **1**. Only one disordered cam ligand component is shown. Thermal ellipsoids are drawn at 50% probability. b) $[\text{Co}_2(\text{DL-cam})_2]_n$ (4,4) grid layer motif in **1**.

Table 2

Selected Bond Distance (Å) and Angle (°) Data for **1**.

Co1–O1 ^{#1}	2.055(3)	O2–Co1–O3 ^{#2}	85.99(13)
Co1–O2	2.008(3)	O2–Co1–O4 ^{#3}	97.18(14)
Co1–O3 ^{#2}	2.146(3)	O2–Co1–N1	96.93(14)
Co1–O4 ^{#3}	2.047(3)	O4 ^{#3} –Co1–O1 ^{#1}	89.37(13)
Co1–N1	2.082(4)	O4 ^{#3} –Co1–O3 ^{#2}	162.66(14)
O1 ^{#1} –Co1–O3 ^{#2}	83.69(13)	O4 ^{#3} –Co1–N1	108.90(14)
O1 ^{#1} –Co1–N1	94.30(13)	N1–Co1–O3 ^{#2}	87.52(14)
O2–Co1–O1 ^{#1}	164.39(13)		

Symmetry transformations: #1 $\times -1, y - 1, z - 1$; #2 $\times, -y + 1/2, z - 1/2$; #3 $-x + 1, y + 1/2, -z + 3/2$

of **1** (25 mg, 16% yield based on Co) were isolated after washing with distilled water, ethanol, and acetone and drying in air. Anal. Calc. for $\text{C}_{34}\text{H}_{46}\text{Co}_2\text{N}_4\text{O}_{12}$ **1**: C, 49.76; H, 5.65; N, 6.83%. Found: C, 50.14; H, 5.48; N, 6.84%. IR (cm^{-1}): 3299 (w), 2960 (w), 1649 (m), 1581 (s), 1550 (s), 1403 (s), 1368 (m), 1325 (m), 1301 (m), 1195 (w), 1167 (w), 1109 (w), 1056 (w), 1038 (w), 887(w), 835 (w), 802 (w), 783 (w), 758 (w), 694 (m)

2.3. Preparation of $[\text{Co}(\text{D-cam})(\text{edin})]_n$ (**2**)

$\text{Co}(\text{NO}_3)_2 \cdot 6\text{H}_2\text{O}$ (107 mg, 0.37 mmol), *D*-camphoric acid (73 mg, 0.37 mmol), and edin (99 mg, 0.37 mmol), and 0.75 mL of a 1.0 M NaOH solution were mixed with 10 mL of distilled H_2O in a 23 mL Teflon-lined acid digestion bomb. The bomb was sealed and heated in an oven at 120 °C for 48 h, and then was cooled slowly to 25 °C. Magenta crystals of **2** (26 mg, 13% yield based on Co) were isolated after washing with distilled water, ethanol, and acetone and drying in

air. Anal. Calc. for $\text{C}_{24}\text{H}_{28}\text{CoN}_4\text{O}_6$ **2**: C, 54.65; H, 5.35; N, 10.62%. Found: C, 54.84; H, 5.29; N, 10.56%. IR (cm^{-1}): 2962(w), 1660(m), 1577(w), 1525(s), 1461(m), 1403(s), 1363(w), 1321(w), 1293(w), 1086(m), 997(w), 861(w), 836(w), 802(s), 697(s), 666(w).

2.4. Preparation of $\{[\text{Co}_2(\text{DL-cam})_2(\text{bdin})] \cdot 2\text{H}_2\text{O}\}_n$ (**3**)

$\text{Co}(\text{NO}_3)_2 \cdot 6\text{H}_2\text{O}$ (107 mg, 0.37 mmol), *D*-camphoric acid (73 mg, 0.37 mmol), and bdin (111 mg, 0.37 mmol), and 0.75 mL of a 1.0 M NaOH solution were mixed with 10 mL of distilled H_2O in a 23 mL Teflon-lined acid digestion bomb. The bomb was sealed and heated in an oven at 120 °C for 48 h, and then was cooled slowly to 25 °C. A few magenta crystals of **3** were found embedded in a large amount of flocculent light pink powder and colorless crystals (presumably unreacted ligands). Multiple attempts at a monophasic preparation of **3** were unfortunately unsuccessful.

2.5. Preparation of $\{[\text{Co}_2(\text{DL-cam})_2(\text{pedin})] \cdot 2\text{H}_2\text{O}\}_n$ (**4**)

$\text{Co}(\text{OAc})_2 \cdot 4\text{H}_2\text{O}$ (92 mg, 0.37 mmol), *D*-camphoric acid (73 mg, 0.37 mmol), and pedin (114 mg, 0.37 mmol), and 0.75 mL of a 1.0 M NaOH solution were mixed with 10 mL of distilled H_2O in a 23 mL Teflon-lined acid digestion bomb. The bomb was sealed and heated in an oven at 120 °C for 48 h, and then was cooled slowly to 25 °C. Magenta crystals of **4** (35 mg, 22% yield based on Co) were isolated after washing with distilled water, ethanol, and acetone and drying in air. Anal. Calc. for $\text{C}_{37}\text{H}_{52}\text{Co}_2\text{N}_4\text{O}_{12}$ **4**: C, 51.51; H, 6.08; N, 6.49%. Found: C, 50.78; H, 6.01; N, 6.13%. IR (cm^{-1}): 3300(w, br), 1674(s), 1540(s), 1415(m), 1301(w), 1053(w), 852(m), 797(w), 764(w),

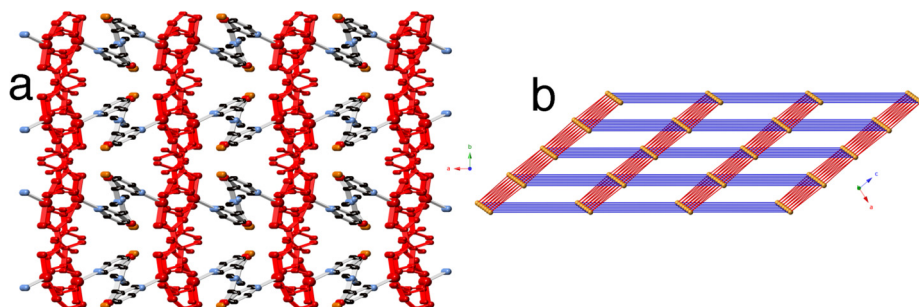


Fig. 2. $[\text{Co}_2(\text{DL-cam})_2(\text{edn})]_n$ 3D coordination polymer network in **1**. $[\text{Co}_2(\text{DL-cam})_2]_n$ layer motifs are shown in red. b) Schematic perspective of the straight-pillared $4^{12}6^3$ pcu net in **1**. Gold spheres represent the centroids of the $\{\text{Co}_2(\text{OCO})_4\}$ paddlewheel dimers. The *DL-cam* and *edn* ligands connections are shown as red and blue rods, respectively. (For interpretation of the references to colour in this figure legend, the reader is referred to the web version of this article.)

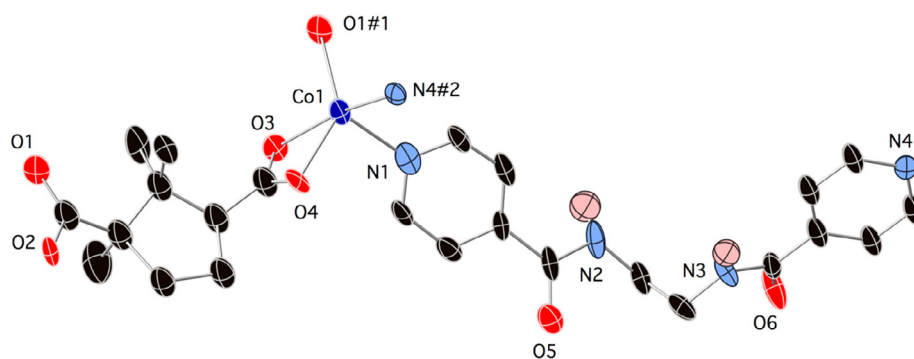


Fig. 3. $\{CoN_2O_3\}$ distorted trigonal bipyramidal coordination environment and complete ligand set in **2**. Thermal ellipsoids are drawn at 50% probability.

Table 3

Selected Bond Distance (Å) and Angle (°) Data for **2**.

Co1–O1 ^{#1}	2.106(15)	O4–Co1–O1 ^{#1}	137.6(5)
Co1–O3	2.131(13)	O4–Co1–O3	63.0(6)
Co1–O4	2.014(14)	O4–Co1–N1	97.8(7)
Co1–N1	2.24(2)	N4 ^{#2} –Co1–O1 ^{#1}	102.1(7)
Co1–N4 ^{#2}	1.973(17)	N4 ^{#2} –Co1–O3	166.8(7)
O1 ^{#1} –Co1–O3	89.4(6)	N4 ^{#2} –Co1–O4	103.8(6)
O1 ^{#1} –Co1–N1	114.7(6)	N4 ^{#2} –Co1–N1	90.9(7)
O3–Co1–N1	90.0(6)		

Symmetry transformations: #1 $-x, y - 1/2, -z + 1$; #2 $-x + 2, y - 1/2, -z + 1$.

684(w).

2.6. Preparation of $[Co(D\text{-cam})(hdin)]_n$ (**5**)

$Co(NO_3)_2 \cdot 6H_2O$ (107 mg, 0.37 mmol), *D*-camphoric acid (73 mg, 0.37 mmol), and *hdin* (119 mg, 0.37 mmol), and 0.75 mL of a 1.0 M NaOH solution were mixed with 10 mL of distilled H_2O in a 23 mL Teflon-lined acid digestion bomb. The bomb was sealed and heated in an oven at 120 °C for 48 h, and then was cooled slowly to 25 °C. Magenta crystals of **5** (41 mg, 19% yield based on Co) were isolated after washing with distilled water, ethanol, and acetone and drying in air. Anal. Calc. for $C_{28}H_{34}CoN_4O_6$ **5**: C, 57.83; H, 5.89; N, 9.63% Found: C, 58.15; H, 6.00; N, 10.37%. IR (cm^{-1}): 2961(w), 1640 (m), 1577(s), 1401(s), 1364(m), 1325(w), 1098(m), 1013(w), 802(m), 698(m).

3. X-ray crystallography

Diffraction data for **1–5** were collected on a Bruker-AXS SMART-CCD X-ray diffractometer using graphite-monochromated Mo-K α

radiation ($\lambda = 0.71073 \text{ \AA}$) at 173 K. The data were processed via SAINT [14], and corrected for both Lorentz and polarization effects and absorption effects using SADABS [15]. The structures were solved using direct methods with SHELXTL [16] within the OLEX2 crystallographic software suite [17]. All non-hydrogen atoms were refined anisotropically. Hydrogen atoms were placed in calculated positions and refined isotropically with a riding model. Crystallographic disorder within the *DL*-camphorate ligands and the aliphatic groups in some of the dipyriddyamide ligands were successfully modeled with partial occupancies and separate parts. The Flack parameters [18] for the crystal structures of **2** and **5** were 0.00(7) and 0.11(2), respectively, indicating excellent to good racemic purity within the crystals. The R_{int} value for the crystal of **2** along with refinement parameters were elevated due to small crystal size with concomitant weak diffraction. Nevertheless the connectivity and topology of compound **2** were unambiguous. Attempts to solve and refine the structures of **2** and **5** in centrosymmetric space groups were unsuccessful; the crystal of **5** showed a small amount of racemic twinning as per the Flack parameter above. Crystallographic details for **1–5** are given in Table 1.

4. Results and discussion

4.1. Synthesis and spectra

Crystalline samples of **1–5** were produced by the hydrothermal reaction of a divalent cobalt salt, *D*-camphoric acid, and the requisite dipyriddyamide ligand in the presence of aqueous base. Unfortunately compound **3** could not be obtained in phase pure fashion after multiple attempts at altering synthetic conditions, which precluded bulk analysis. The infrared spectra of **1–2** and **4–5** were consistent with their structural components as determined by single-crystal X-ray diffraction.

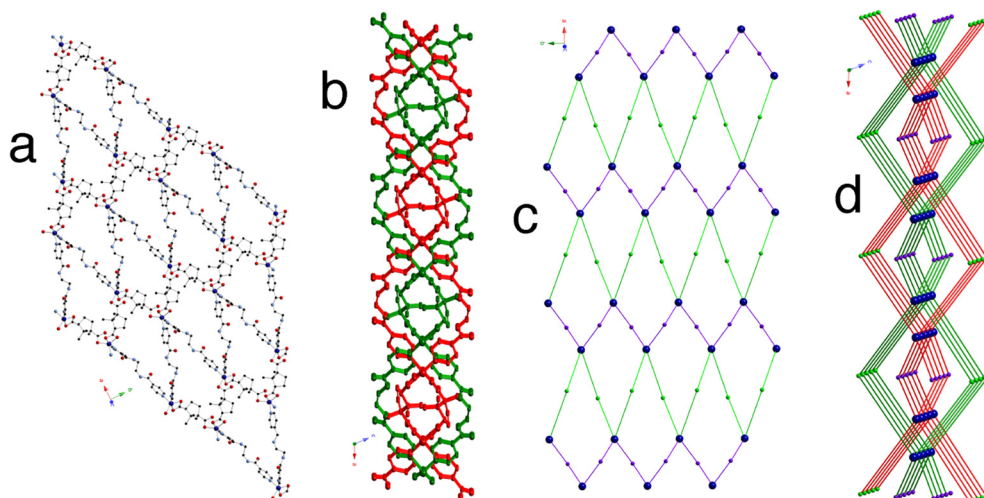


Fig. 4. a) $[Co(DL\text{-cam})(edin)]_n$ (4,4) grid layer motif in **2**. b) Side view of the 2-fold parallel interpenetration of $[Co(DL\text{-cam})(edin)]_n$ layer motifs in **2**. c) Schematic perspective of the looped $(8)_2(8^4)12^2$ topology net invoked for **2**. The purple and green rods represent the *DL*-cam and *edin* loops, respectively. d) Two-fold parallel interpenetration of looped nets in **2**, with *DL*-cam and *edin* ligands acting as loops instead of straight linkers in order to avoid edge crossing. (For interpretation of the references to colour in this figure legend, the reader is referred to the web version of this article.)

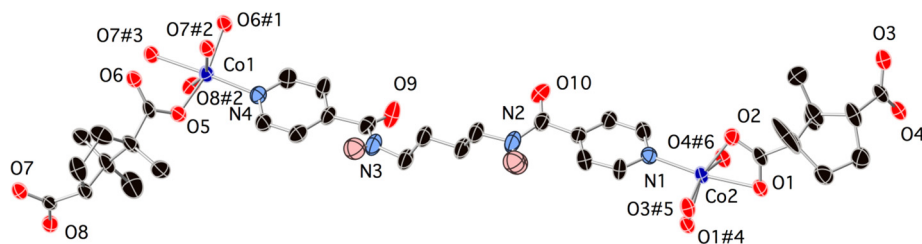


Fig. 5. $\{\text{CoNO}_4\}$ square pyramidal coordination environment and complete ligand set in **3**. Thermal ellipsoids are drawn at 50% probability.

Table 4

Selected Bond Distance (Å) and Angle (°) Data for **3**.

Co1–O5	2.022(4)	O7 ^{#2} –Co1–O7	101.02(14)
Co1–O6 ^{#1}	2.021(4)	O8 ^{#2} –Co1–O7 ^{#2}	60.30(17)
Co1–O7 ^{#2}	2.277(4)	O8 ^{#2} –Co1–O7	160.88(17)
Co1–O7 ^{#3}	2.256(5)	O8 ^{#2} –Co1–N4	111.0(2)
Co1–O8 ^{#2}	2.073(5)	N4–Co1–O7	87.68(19)
Co1–N4	2.093(5)	N4–Co1–O7	171.27(19)
Co2–O1	2.275(4)	O1 ^{#4} –Co2–O1	100.90(15)
Co2–O1 ^{#4}	2.263(5)	O2–Co2–O1	60.33(17)
Co2–O2	2.065(5)	O2–Co2–O1 ^{#4}	160.75(17)
Co2–O3 ^{#5}	2.021(4)	O2–Co2–N1	111.1(2)
Co2–O4 ^{#6}	2.018(4)	O3 ^{#5} –Co2–O1 ^{#4}	83.21(17)
Co2–N1	2.093(5)	O3 ^{#5} –Co2–O1	85.51(17)
O5–Co1–O7 ^{#2}	85.92(16)	O3 ^{#5} –Co2–O2	98.48(19)
O5–Co1–O7 ^{#2}	83.21(17)	O3 ^{#5} –Co2–N1	96.1(2)
O5–Co1–O8 ^{#2}	98.41(19)	O4 ^{#6} –Co2–O1 ^{#4}	81.98(17)
O5–Co1–N4	96.0(2)	O4 ^{#6} –Co2–O1	85.39(17)
O6 ^{#1} –Co1–O5	161.15(19)	O4 ^{#6} –Co2–O2	91.60(18)
O6 ^{#1} –Co1–O7 ^{#2}	85.26(17)	O4 ^{#6} –Co2–O3 ^{#5}	160.8(2)
O6 ^{#1} –Co1–O7 ^{#3}	82.18(17)	O4 ^{#6} –Co2–N1	95.4(2)
O6 ^{#1} –Co1–O8 ^{#2}	91.61(18)	N1–Co2–O1	171.43(19)
O6 ^{#1} –Co1–N4	95.3(2)	N1–Co2–O1 ^{#4}	87.66(19)

Symmetry transformations: #1 $-x + 1, -y + 3, -z + 1$; #2 $x, -y + 7/2, z - 1/2$; #3 $-x + 1, y - 1/2, -z + 3/2$; #4 $-x + 2, -y, -z + 1$; #5 $x, -y - 1/2, z + 1/2$; #6 $-x + 2, y + 1/2, -z + 1/2$

Intense, broad asymmetric and symmetric C–O stretching bands within the camphorate ligands were observed at 1550 and 1403 cm^{-1} for **1**, 1525 and 1403 cm^{-1} for **2**, at 1540 and 1415 cm^{-1} for **4**, and at 1577 and 1401 cm^{-1} for **5**. Moderate intensity bands in the range of $\sim 1600\text{ cm}^{-1}$ to $\sim 1300\text{ cm}^{-1}$ are attributed to the stretching modes of the pyridyl rings of the dipyriddyamide ligands [19]. Features corresponding to C–H bending and ring puckering within the pyridyl moieties exist in the region between ~ 900 and $\sim 650\text{ cm}^{-1}$. Broad, weak spectral bands in the vicinity of $\sim 3000\text{--}3400\text{ cm}^{-1}$ indicate the presence of unbound water molecules in the spectra of **1** and **4**. The carbonyl stretching bands for the dipyriddyamide ligands appeared at 1649 cm^{-1} for **1**, 1660 cm^{-1} for **2**, 1674 cm^{-1} for **4**, and 1640 cm^{-1} for **5**.

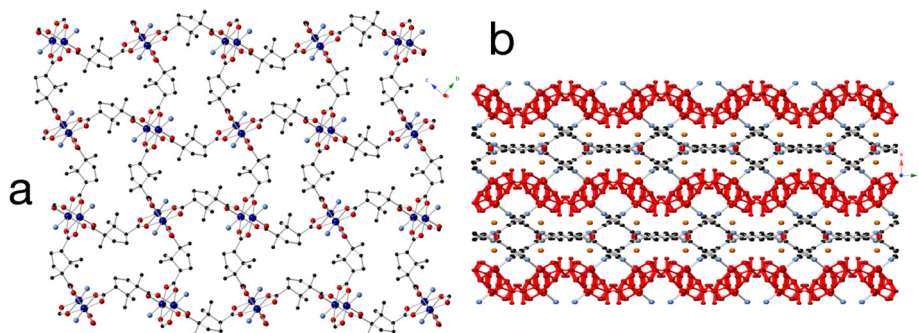


Fig. 6. a) b) $[\text{Co}_2(\text{DL-cam})_2]_n$ (4,4) grid layer motif in **3**. b) $[\text{Co}_2(\text{DL-cam})_2(\text{bdin})]_n$ 3D coordination polymer network in **3**. $[\text{Co}_2(\text{DL-cam})_2]_n$ layer motifs are shown in red with cross-pillaring bdin ligands situated between the layers. (For interpretation of the references to colour in this figure legend, the reader is referred to the web version of this article.)

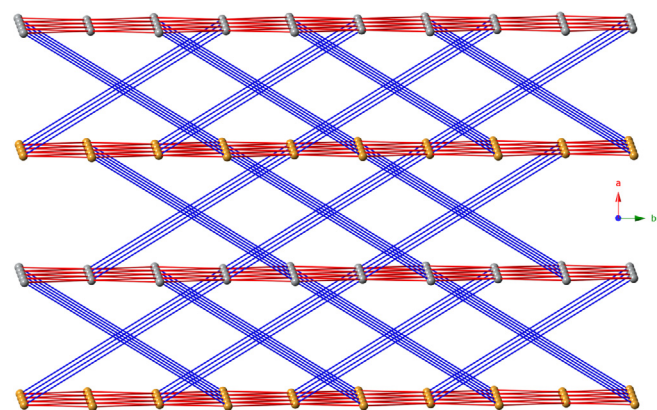


Fig. 7. Schematic perspective of the rare cross-pillared self-penetrated $4^6 108$ roa net in **3** and **4**. Gold and silver spheres represent the centroids of the $\{\text{Co}_2(\text{OCO})_4\}$ paddlewheel dimers. The DL-cam and dipyriddyamide ligand connections are shown as red and blue rods, respectively. (For interpretation of the references to colour in this figure legend, the reader is referred to the web version of this article.)

4.2. Structural description of $\{[\text{Co}_2(\text{DL-cam})_2(\text{edn})] \cdot 2\text{H}_2\text{O}\}_n$ (**1**)

The asymmetric unit of compound **1** consists of a divalent cobalt atom, a camphorate ligand with a methyl group disordered equally over two sets of positions, revealing the presence of both *D*-cam and *L*-cam ligands in a racemic 50:50 ratio, half of an edn ligand whose central C–C σ bond rests over a crystallographic inversion center, and a water molecule of crystallization. A $\{\text{CoO}_4\text{N}\}$ square pyramidal coordination environment (Fig. 1a) with a τ value of 0.028 [20] is evident at cobalt, with single carboxylate oxygen atom donors from four DL-cam ligands in the basal plane. The apical position is taken up by a pyridyl nitrogen donor atom from an edn ligand. Bond lengths and angles within the coordination environment are listed in Table 2.

The DL-cam ligands adopt a bis-bridging exotetradentate binding mode. Thus $\{\text{Co}_2(\text{OCO})_4\}$ paddlewheel dimeric units are constructed with a Co–Co internuclear distance of $2.736(1)\text{ \AA}$ spanned by *syn-syn* bridging carboxylates from four DL-cam ligands. The full span of the DL-cam ligands forms $[\text{Co}_2(\text{DL-cam})_2]_n$ coordination polymer layer motifs that are oriented along the *bc* crystal planes (Fig. 1b). The shortest

Table 5
Selected Bond Distance (Å) and Angle (°) Data for 4.

Co1–O3 ^{#1}	2.286(5)	O8–Co1–O3 ^{#1}	83.6(2)
Co1–O3 ^{#2}	2.278(5)	O8–Co1–O4 ^{#2}	96.9(2)
Co1–O4 ^{#2}	2.070(5)	O8–Co1–O7 ^{#3}	161.4(2)
Co1–O7 ^{#3}	2.012(5)	O8–Co1–N1	94.9(2)
Co1–O8	2.007(5)	N1–Co1–O3 ^{#1}	88.0(2)
Co1–N1	2.081(6)	N1–Co1–O3 ^{#2}	169.8(2)
Co2–O1 ^{#4}	2.020(5)	O1 ^{#4} –Co2–O5 ^{#4}	82.4(2)
Co2–O2	2.019(5)	O1 ^{#4} –Co2–O5	86.08(19)
Co2–O5	2.288(5)	O1 ^{#4} –Co2–O6	92.8(2)
Co2–O5 ^{#4}	2.264(5)	O1 ^{#4} –Co2–N4 ^{#5}	96.3(2)
Co2–O6	2.071(6)	O2–Co2–O1 ^{#4}	161.3(2)
Co2–N4 ^{#5}	2.088(6)	O2–Co2–O5	84.79(18)
O3 ^{#2} –Co1–O3 ^{#1}	102.23(15)	O2–Co2–O5 ^{#4}	83.7(2)
O4 ^{#2} –Co1–O3	60.2(2)	O2–Co2–O6	96.7(2)
O4 ^{#2} –Co1–O3 ^{#1}	162.2(2)	O2–Co2–N4 ^{#5}	95.6(2)
O4 ^{#2} –Co1–N1	109.7(2)	O5 ^{#4} –Co2–O5	102.36(15)
O7 ^{#3} –Co1–O3 ^{#2}	85.84(19)	O6–Co2–O5	60.0(2)
O7 ^{#3} –Co1–O3 ^{#1}	82.3(2)	O6–Co2–O5 ^{#4}	162.1(2)
O7 ^{#3} –Co1–O4 ^{#2}	92.9(2)	O6–Co2–N4 ^{#5}	109.9(2)
O7 ^{#3} –Co1–N1	96.7(2)	N4 ^{#5} –Co2–O5 ^{#4}	87.8(2)
O8–Co1–O3 ^{#2}	85.36(19)	N4 ^{#5} –Co2–O5	169.8(2)

Symmetry transformations: #1 $-x + 2, -y + 1, -z + 1$; #2 $x, y, z - 1$; #3 $-x + 2, -y + 1, -z$; #4 $-x + 3, -y + 1, -z + 1$; #5 $x + 2, -y + 1/2, z + 1/2$.

Co··Co distances through the *DL*-cam ligands measure 9.249(7) and 9.703(7) Å. Adjacent [Co₂(*DL*-cam)₂]_n layer motifs in **1** are pillared in the *a* crystal direction by dipodal edn ligands to construct a non-interpenetrated 3D {[Co₂(*DL*-cam)₂(edn)]_n network (Fig. 2a). The edn ligands adopt an *anti* conformation with their pyridyl rings pointing in opposite directions, and span a Co··Co distance of 14.00(1) Å. Treating the {Co₂(OCO)₄} paddlewheels as 6-connected nodes reveals a straight-pillared 4¹²6³ *pcu* network (Fig. 2b) according to TOPOS [21]. The water molecules of crystallization are held to the 3D network, and situated between the [Co₂(*DL*-cam)₂]_n layer submotifs, by hydrogen bonding donation to edn carbonyl oxygen atoms (Table S1).

4.3. Structural description of [Co(*D*-cam)(edn)]_n (**2**)

The asymmetric unit of compound **2** contains a divalent cobalt atom, a *D*-cam ligand, and an edn ligand. A distorted five-coordinate {CoN₂O₃} coordination sphere is observed at cobalt, with a τ trigonality factor of 0.48 indicative of a hybrid of square pyramidal and trigonal bipyramidal coordination geometries (Fig. 3). If a trigonal bipyramidal coordination sphere is invoked, a carboxylate group from a *D*-cam ligand spans an axial and an equatorial position, with a pyridyl nitrogen donor atom from an edn ligand also in an axial position. The other two remaining coordination sites in the equatorial plane contain a pyridyl nitrogen donor atom from a second edn ligand and a carboxylate

Table 6
Selected Bond Distance (Å) and Angle (°) Data for 5.

Co1–O3	2.015(9)	O4–Co1–O4 ^{#1}	98.7(5)
Co1–O3 ^{#1}	2.015(9)	N1 ^{#1} –Co1–O4	156.1(4)
Co1–O4 ^{#1}	2.295(9)	N1–Co1–O4 ^{#1}	156.1(4)
Co1–O4	2.295(9)	N1–Co1–O4	88.0(3)
Co1–N1	2.151(10)	N1 ^{#1} –Co1–O4 ^{#1}	88.0(3)
Co1–N1 ^{#1}	2.151(10)	N1–Co1–N1	95.1(5)
Co2–O5 ^{#2}	2.121(11)	O5 ^{#2} –Co2–O5	107.2(6)
Co2–O5	2.121(11)	O5–Co2–O6	60.9(3)
Co2–O6	2.202(10)	O5 ^{#2} –Co2–O6	96.1(4)
Co2–O6 ^{#2}	2.202(10)	O5 ^{#2} –Co2–O6 ^{#2}	60.9(3)
Co2–N2	2.117(10)	O5–Co2–O6 ^{#2}	96.1(4)
Co2–N2 ^{#2}	2.116(10)	O6 ^{#2} –Co2–O6	142.7(6)
O3–Co1–O3 ^{#1}	142.9(6)	N2 ^{#2} –Co2–O5 ^{#2}	90.0(4)
O3–Co1–O4 ^{#1}	94.9(4)	N2–Co2–O5 ^{#2}	148.1(4)
O3 ^{#1} –Co1–O4 ^{#1}	60.0(4)	N2–Co2–O5	90.0(4)
O3 ^{#1} –Co1–O4	94.9(4)	N2 ^{#2} –Co2–O5	148.1(4)
O3–Co1–O4	60.0(4)	N2–Co2–O6 ^{#2}	91.3(4)
O3–Co1–N1	108.2(4)	N2 ^{#2} –Co2–O6	91.3(4)
O3 ^{#1} –Co1–N1	96.8(4)	N2 ^{#2} –Co2–O6 ^{#2}	115.7(4)
O3–Co1–N1 ^{#1}	96.8(4)	N2–Co2–O6	115.7(4)
O3 ^{#1} –Co1–N1 ^{#1}	108.2(4)	N2 ^{#2} –Co2–N2	88.7(5)

Symmetry transformations: #1 $-x + 2, -y, z$; #2 $-x + 1, -y + 1, z$.

oxygen atom donor from a second *D*-cam ligand. Thus the two pyridyl donor atoms are oriented in a *cis* fashion with respect to each other. Bond lengths and angles within the distorted coordination sphere are listed in Table 3.

The *D*-cam ligands in **2** adopt a chelating/monodentate binding mode and construct zig-zag [Co(*D*-cam)]_n coordination polymer chains that are oriented along the *b* crystal direction, with a Co··Co through-ligand distance of 8.916(7) Å. These are pillared by *cis*-disposed dipodal edn ligands with a Co··Co distance of 14.87(1) Å to construct [Co(*D*-cam)(edn)]_n grid-like coordination polymer layers (Fig. 4a). The grid apertures in **2** are large enough to accommodate interpenetration of a second [Co(*D*-cam)(edn)]_n layer motif along the *ab* crystal planes as shown in Fig. 4b. While the grid-like layers in **2** appear to have a common 4-connected (4,4) grid topology, such a topology would enforce edge-crossing within an interpenetrated pair of layers. Therefore, according to the nomenclature of Batten et al. [22], each *D*-cam and edn ligand in **2** is considered to be a 2-connected node in a looped net with the cobalt atoms representing 4-connected nodes. According to TOPOS, the 2,2,4-connected layer of **2** has a (8)₂(8⁴12²) topology (Fig. 4c). A side view of the two-fold interpenetrated system of looped layers in **2** is shown in Fig. 4d. Sets of interpenetrated layers aggregate along the *c* crystal direction by means of non-classical C–H··O interactions between edn central ethylene units and edn C=O moieties (Fig. S1).

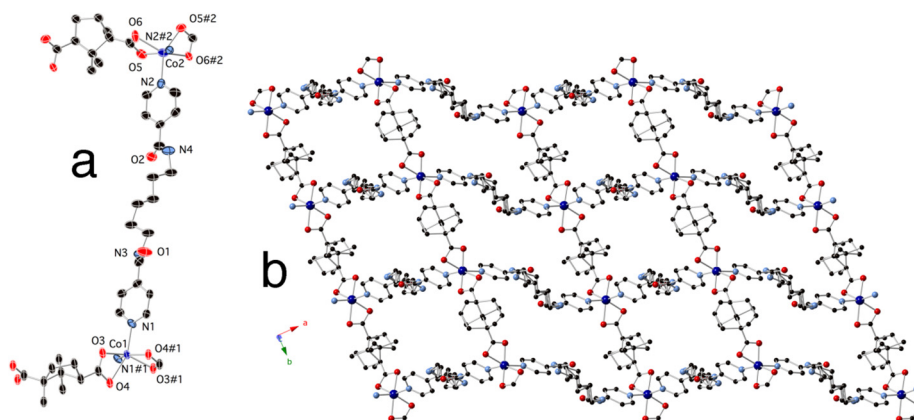


Fig. 8. a) {CoO₄N₂} octahedral coordination environment and complete ligand set in **5**. Thermal ellipsoids are drawn at 50% probability. Only one disordered conformation of each ligand is shown. b) Sawtooth [Co(*D*-cam)(hdn)]_n (4,4) grid layer motif in **5**. Both disordered conformations of each ligand set are shown.

4.4. Structural description of $\{[Co_2(DL\text{-cam})_2(bdin)]\cdot 2H_2O\}_n$ (3)

The asymmetric unit of compound **3** contains two divalent cobalt atoms (Co1, Co2), two racemized *DL*-cam ligands, a complete *bdin* ligand, and two water molecules of crystallization. Each cobalt atom shows a distorted $\{CoNO_5\}$ coordination octahedron (Fig. 5) with a chelating carboxylate group from one *DL*-cam ligand and monodentate oxygen atom donors from three other *DL*-cam ligands, along with a pyridyl nitrogen donor atom from a *bdin* ligand. Bond lengths and angles within the coordination environments are listed in Table 4.

Both of the crystallographically distinct *DL*-cam ligands adopt an exotetradentate $\mu_4\text{-}\kappa^4\text{-O,O':O':O''O'''}$ binding mode in which one carboxylate group chelates to a cobalt atom while binding in a monodentate fashion to another, with the other carboxylate terminus bridging two cobalt atoms in a *syn-syn* fashion. As a result $\{Co_2(OCO)_4\}$ paddlewheel dimeric units are formed in **3**, with Co1...Co1 distances of 2.883(2) Å and Co2...Co2 distances of 2.890(2) Å.

The $\{Co_2(OCO)_4\}$ paddlewheel dimers are connected by the full span of the *DL*-cam ligands to generate undulating $[Co_2(DL\text{-cam})_2]_n$ coordination polymer grid-like layers that are oriented parallel to the *bc* crystal planes (Fig. 6a).

The Co1-based $[Co_2(DL\text{-cam})_2]_n$ layers and the Co2-based $[Co_2(DL\text{-cam})_2]_n$ layers are pillared by dipodal *bdin* ligands into a $[Co_2(DL\text{-cam})_2(bdin)]_n$ 3D coordination polymer network (Fig. 6b). The *bdin* ligands have a splayed-open anti conformation of their central aliphatic tethers (torsion angle = 162.8°) and span a Co...Co distance of 19.926(6) Å. As this distance is substantially longer than that spanned by the *edn* ligands in **1**, a straight-pillared $4^{12}6^3$ *pcu* network is not formed in **3**. Instead, by treating the $\{Co_2(OCO)_4\}$ paddlewheel dimers as 6-connected nodes, a very rare $4^46^{10}8$ *roa* cross-pillared self-penetrated network can be invoked (Fig. 7). Water molecules of crystallization are anchored to the coordination polymer network of **3** by accepting hydrogen bonding from *bdin* N–H groups and by donating hydrogen bonds to the *bdin* C=O groups (Table S1).

4.5. Structural description of $\{[Co_2(DL\text{-cam})_2(pedin)]\cdot 2H_2O\}_n$ (4)

The asymmetric unit of compound **4** contains two divalent cobalt atoms (Co1, Co2), two racemized *DL*-cam ligands, a complete *pedin* ligand, and two water molecules of crystallization. As in **3**, a distorted $\{CoNO_5\}$ coordination octahedral geometry is in evidence at each cobalt atom in **4** (Fig. S2). Bond lengths and angles within the coordination spheres are listed in Table 5. The salient structural features of **4**, namely $[Co_2(DL\text{-cam})_2]_n$ layers constructed from $\{Co_2(OCO)_4\}$ paddlewheel dimers, further pillared by dipodal *pedin* ligands into a $[Co_2(DL\text{-cam})_2(pedin)]_n$ 3D coordination polymer net, are similar to that of **3**. The *pedin* ligands in **4** adopt an *anti-anti* conformation of their central pentamethylene tethers and span a Co...Co distance of 20.435(1) Å. The resulting 6-connected net in **4** has a $4^46^{10}8$ *roa* cross-pillared self-penetrated network as seen in **3** (Fig. 7).

4.6. Structural description of $[Co(D\text{-cam})(hdin)]_n$ (5)

The asymmetric unit of compound **5** contains a divalent cobalt atom, a *D*-cam ligand disordered over two sets of positions and a *hdin* ligand disordered over two sets of positions. A distorted octahedral $\{CoN_2O_4\}$ coordination geometry is observed at each cobalt atom, with chelating carboxylate groups from two *D*-cam ligands comprising four of the coordination sites (Fig. 8a). The remaining two *cis* disposed coordination sites are taken up by pyridyl nitrogen donor atoms from two *hdin* ligands. Bond lengths and angles within the octahedral coordination sphere are listed in Table 6.

Bis(chelating) *D*-cam ligands connect the cobalt atoms into $[Co(D\text{-cam})]_n$ coordination polymer chains that are oriented along the *b* crystal direction with a Co...Co through-ligand distance of 9.241(2) Å that denotes the *b* lattice parameter. The $[Co(D\text{-cam})]_n$ chain submotifs

are pillared by the *hdin* ligands into sawtooth $[Co(D\text{-cam})(hdin)]_n$ coordination polymer layers (Fig. 8b). The *hdin* ligands span a Co...Co distance of 22.365(5) Å; the *cis*-disposition of the pyridyl nitrogen donor atoms of the *hdin* ligands enforce the sharp sawtooth morphology of the layer motifs. Adjacent $[Co(D\text{-cam})(hdin)]_n$ coordination polymer sawtooth layers stack in an *ABAB* pattern along the *c* crystal direction (Fig. S3) by means of hydrogen bonding donation from *hdin* N–H groups to bound *D*-cam carboxylate oxygen atoms.

4.7. Thermal properties

Compound **1** underwent loss of its co-crystallized water molecules between ~30 and ~125 °C, with a mass loss of 4.5% matching well with the predicted value for elimination of two molar equivalents of water. Ligand combustion occurred above ~260 °C. Compound **2** underwent combustion above 340 °C. Compound **4** lost its water molecules of crystallization upon long term storage, and the framework itself combusted above 300 °C. Compound **5** underwent combustion above 270 °C. The TGA traces for **1–2** and **4–5** are shown in Figs. S4–S7, respectively.

5. Conclusions

A wide variety of coligand dependent structural topologies, including two rare examples of a cross-pillared *roa* self-penetrated topology and an intriguing looped layer network, has been obtained in a series of cobalt camphorate coordination polymers. No clear structural trends can be identified upon lengthening the central aliphatic tether of the neutral dipyridylamide coligands. All of the 3D coordination polymer phases exhibit scrambling of the original *D*-camphorate chirality. The self-penetrated *roa* topology shows the highest thermal robustness of the coordination polymers in this series.

Acknowledgements

Support for this work was provided by the Honors College of Michigan State University. J.J.P.'s research fellowship was provided by the Michigan State University Chemistry Department's National Science Foundation REU Program under award number CHE-1358842.

Appendix A. Supplementary data

Supplementary data (Hydrogen bonding information, additional molecular graphics, and thermogravimetric analysis plots. Crystallographic data (excluding structure factors) for **1–5** have been deposited with the Cambridge Crystallographic Data Centre with Nos. 1824082–1824086, respectively. Copies of the data can be obtained free of charge via the Internet at < <https://summary.ccdc.cam.ac.uk/structure-summary-form> > to this article can be found online at <https://doi.org/10.1016/j.ica.2019.119087>.

References

- [1] D.W. Lim, S.A. Chyun, M.P. Suh, *Angew. Chem. Int. Ed.* **53** (2014) 7819.
- [2] J.S. Wright, I.J. Vitórica-Yrezábal, S.P. Thompson, L. Brammer, *Chem. Eur. J.* **22** (2016) 13120.
- [3] L.L. Lv, J. Yang, H.M. Zhang, Y.Y. Liu, J.F. Ma, *Inorg. Chem.* **54** (2015) 1744.
- [4] Y.B. Huang, Q. Wang, J. Liang, X. Wang, R. Cao, *J. Am. Chem. Soc.* **138** (2016) 10104.
- [5] L. Guan, Y. Wang, *J. Solid State Chem.* **230** (2015) 243.
- [6] (a) Z. Hu, B.J. Deibert, J. Li, *Chem. Soc. Rev.* **43** (2014) 5815; (b) G. Wang, L. Yang, Y. Li, H. Song, W. Ruan, Z. Chang, X. Bu, *Dalton Trans.* **42** (2013) 12865.
- [7] I. Imaz, M. Rubio-Martinez, L. Garcia-Fernandez, F. Garcia, D. Ruiz-Molina, J. Hernando, V. Puentes, D. MasPOCH, *Chem. Commun.* **46** (2010) 4737.
- [8] (a) C. Wu, W. Lin, *Angew. Chem., Int. Ed.* **46** (2007) 1075; (b) R. Vaidhyanathan, D. Bradshaw, J. Rebilly, J. Barrio, J.A. Gould, N. Berry, M. Rosseinsky, *Angew. Chem., Int. Ed.* **45** (2006) 6495.
- [9] J. Zhang, E. Chew, S. Chen, J.T.H. Pham, X. Bu, *Inorg. Chem.* **47** (2008) 3495.

- [10] (a) J. Zhang, X. Bu, *Chem. Commun.* (2008) 444;
(b) J. Zhang, X. Bu, *Chem. Commun.* (2009) 206.
- [11] K.M. Blake, C.M. Gandolfo, J.W. Uebler, R.L. LaDuca, *Cryst. Growth Des.* 12 (2012) 5125.
- [12] J.J. Przybyla, R.L. LaDuca, *CrystEngComm* 20 (2018) 280.
- [13] T.S. Gardner, E. Wenis, J.J. Lee, *J. Org. Chem.* 19 (1954) 753.
- [14] SAINT, Software for Data Extraction and Reduction, Version 6.02, Bruker AXS Inc., Madison, WI, 2002.
- [15] SADABS, Software for Empirical Absorption Correction. Version 2.03, Bruker AXS Inc., Madison, WI, 2002.
- [16] G.M. Sheldrick, SHELXTL, Program for Crystal Structure Refinement, University of Göttingen, Göttingen, Germany, 1997.
- [17] O.V. Dolomanov, L.J. Bourhis, R.J. Gildea, J.A.K. Howard, H. Puschmann, *J. Appl. Cryst.* 42 (2009) 229.
- [18] H.D. Flack, *Acta Crystallogr. A* 29 (1983) 876.
- [19] M. Kurmoo, C. Estournes, Y. Oka, H. Kumagai, K. Inoue, *Inorg. Chem.* 44 (2005) 217.
- [20] A.W. Addison, T.N.J. Rao, *J. Chem. Soc., Dalton Trans.* (1984) 1349.
- [21] V.A. Blatov, A.P. Shevchenko, D.M. Proserpio, *Cryst. Growth Des.* 14 (2014) 3576. TOPOS software is available for download at: < <http://www.topospro.com> >.